Eur. Phys. J. B **7**, 9–17 (1999)

THE EUROPEAN PHYSICAL JOURNAL B

EDP Sciences

^{27}Al Nuclear Magnetic Resonance studies of $CeAuAl_3$

P. Vonlanthen, J.L. Gavilano, B. Ambrosini, and H.R. Ott[a]

Laboratorium für Festkörperphysik, Eidgenössische Technische Hochschule-Hönggerberg, 8093 Zürich, Switzerland

Received: 5 May 1998 / Received in final form: 16 July 1998 / Accepted: 20 July 1998

Abstract. We report ^{27}Al Nuclear Magnetic Resonance studies of $CeAuAl_3$ and $LaAuAl_3$ at frequencies between 1.30 and 76.91 MHz and at temperatures from 45 mK up to 320 K. $CeAuAl_3$ is a new heavy-electron compound which orders antiferromagnetically at 1.32 K. For the two inequivalent Al sites of $CeAuAl_3$, the transferred hyperfine couplings $H_{hf} = 1.91$ kOe/μ_B and $H_{hf} = 2.40$ kOe/μ_B are relatively small compared to those in other Ce compounds. The nuclear quadrupolar coupling constants e^2qQ/h are 2.9 MHz and 7.8 MHz, respectively. We suggest that the magnetic structure of the ordered state below 1.32 K is of a simple spiral type with the ordered Ce moments arranged ferromagnetically within the (ab) planes of the tetragonal crystal lattice. Based on this magnetic structure we estimate a 25% reduction of the Ce moments, most likely due to Kondo screening. At high temperatures, in the paramagnetic state of $CeAuAl_3$, the spin-lattice relaxation rate T_1^{-1} is dominated by the fluctuations of the localised Ce moments. At 20 K, T_1^{-1} is 96 s^{-1}, more than two orders of magnitude larger than for the reference compound $LaAuAl_3$. For temperatures lower than 20 K T_1^{-1} decreases as a function of (T/H) and below 1 K, displays a linear-in-T behaviour, strongly enhanced compared to the reference compound $LaAuAl_3$.

PACS. 75.20.Hr Local moment in compounds and alloys; Kondo effect, valence fluctuations, heavy fermions – 75.30.-m Intrinsic properties of magnetically ordered materials – 76.60.-k Nuclear magnetic resonance and relaxation

1 Introduction

$CeAuAl_3$ is an intermetallic compound [1] whose thermal and transport properties at low temperature suggest the presence of strongly correlated electrons in a magnetically ordered phase [2]. Anomalies in the specific heat $C_p(T)$, the magnetic susceptibility $\chi(T)$ and the electrical resistivity $\rho(T)$ of $CeAuAl_3$ indicate a cooperative phase transition at $T_N = 1.32$ K to an antiferromagnetically ordered state.

Below T_N, C_p is well approximated by $C_p = a_N T^{-2} + \gamma T + a_m T^3$ with $a_N = 41$ μJK/mol, $\gamma = 227$ mJ/molK^2, and $a_m = 10.1$ J/molK^4. In reference [2] the T^{-2} term was assumed to be of nuclear origin and the T^3 term was identified with the expected contribution of spin-wave excitations in the magnetically ordered state. The large linear-in-T term suggests the presence of strongly-correlated electrons in the magnetically ordered state. Since the entropy reaches a value of $R\ln(2)$ at approximately 4.5 K it has been suggested [2] that the transition at $T_N = 1.32$ occurs within a doublet crystal-field ground state of the Ce $4f$-electrons. This is consistent with the results for the magnetic susceptibility which can be explained by assuming that the doublet $J_Z = \pm 1/2$ is the crystal-field ground state, with the first excited doublet at 58 K above the ground state. For $T > 200$, $\chi(T)$ can be approximated by a Curie-Weiss law with an effective magnetic moment close to the value of a free Ce^{3+} ion. Since the susceptibility of the reference compound $LaAuAl_3$ is very small, the measured susceptibility of $CeAuAl_3$ can safely be identified as being due to the f-electron susceptibility χ_f.

Below 1 K, the electrical resistivity $\rho(T)$ is well approximated by $\rho(T) = \rho_0 + AT^2$, with $\rho_0 = 56.5$ $\mu\Omega$cm and a large prefactor $A = 5.0$ $\mu\Omega$cm/K^2. The T^2 contribution to $\rho(T)$ provides further evidence for the presence of strongly correlated electrons coexisting with the antiferromagnetically ordered state.

$CeAuAl_3$ crystallizes with a structure of the $BaNiSn_3$-type, belonging to the $I4mm$ space group [1]. This structure is tetragonal with 2 formula units per unit cell with lattice parameters $a = 4.3318(2)$ Å and $c = 10.8390(7)$ Å. $CeAuAl_3$ has a single Ce site with the $4mm$ point-group symmetry and therefore, the Ce^{3+} $4f$-electron $J = 5/2$ ground state is split by the crystal electric-field into three doublets. Each Ce atom has four Ce nearest neighbors in the same (001) plane at a distance of 4.3318 Å. There are two inequivalent Al sites, denoted here as Al_1 and Al_2. One of the Al sites (Al_1) has the $4mm$ point-group symmetry and four Ce nearest neighbors at a distance of 3.17 Å. The second Al site (Al_2) has the mm point-group symmetry and four Ce nearest neighbors at a distance of 3.46 Å.

The reference compound $LaAuAl_3$ has the same crystal structure as $CeAuAl_3$, with the lattice parameters

[a] e-mail: ott@solid.phys.ethz.ch

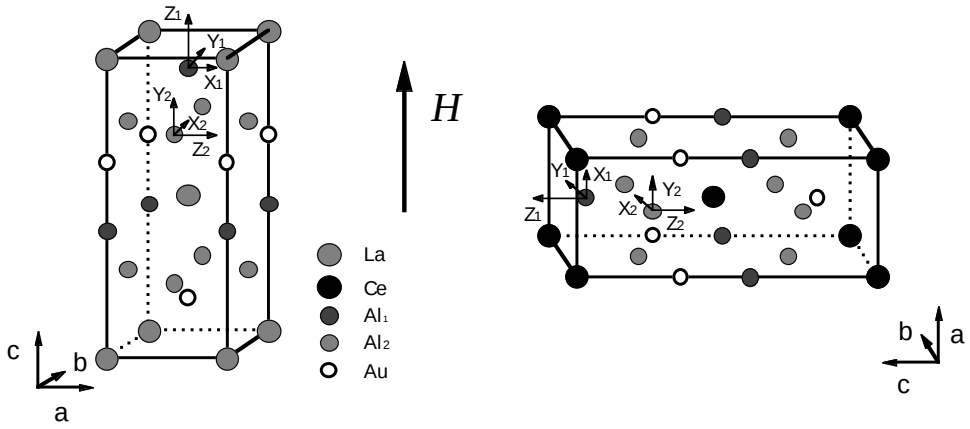

Fig. 1. Crystallographic unit cells of $LaAuAl_3$ (left) and $CeAuAl_3$ (right). The main axis for the electrical field gradients at the Al sites are indicated by the coordinate axis with the convention $|V_{ZZ}| \geq |V_{YY}| \geq |V_{XX}|$. The arrow shows the direction of the applied field responsible for the orientation of the crystallites, which here is indicated by the positions of the unit cells (see text).

$a = 4.3660$ Å and $c = 10.8445$ Å and, apart from the Ce $4f$-electrons, similar electronic configurations are expected for both compounds.

2 Experimental aspects

2.1 Samples and facilities

Our polycrystalline $CeAuAl_3$ and $LaAuAl_3$ materials were synthesized in an argon arc furnace, and they were subsequently annealed for one month at 750 °C and at 735 °C respectively. All our NMR measurements were performed on powdered samples, with grains of linear dimensions smaller than 30 μm, prepared using material from the same batches used for investigating thermodynamic and transport properties [2]. The measurements above 4 K were performed in a ^{4}He flow cryostat equipped with a superconducting 8.5 Tesla magnet, the sample being placed directly into the flowing ^{4}He gas. Below 4 K the measurements were performed in a ^{3}He-^{4}He dilution refrigerator equipped with a superconducting 8 Tesla magnet, the sample being immersed into the ^{3}He-^{4}He mixture. The samples were oriented by the application of magnetic fields of the order of 5 Tesla at $T \leq 20$ K. In the case of $LaAuAl_3$ the c-axis of the crystallites was found to be oriented along the magnetic field, but in the case of $CeAuAl_3$, due to the fact that $J_Z = \pm 1/2$ is the crystal-field ground state of the Ce $4f$-electrons, the c-axis of the crystallites was oriented perpendicularly to the applied magnetic field as shown in Figure 1.

2.2 Measurement techniques

The NMR spectra at fixed frequencies were obtained by integrating spin-echo intensities at a given external magnetic field and changing stepwise the magnetic field. The ^{27}Al NMR measurements of $CeAuAl_3$ and $LaAuAl_3$ were performed at temperatures between 45 mK and 320 K at frequencies between 1.30 MHz and 76.91 MHz.

The spin-lattice relaxation rate T_1^{-1} was measured as follows. First we rotated the nuclear magnetisation out of equilibrium by irradiating the $+1/2 \leftrightarrow -1/2$ nuclear Zeeman transition with either a single rf pulse (fast irradiation) or a long comb of rf pulses (slow irradiation). After a variable recovery time t we measured the integrated spin-echo intensity $m(t)$. The expected functional form of $m(t)$ for the central transition of the ^{27}Al nuclei is a sum of three exponentials [3]

$$1 - \frac{m(t)}{m(\infty)} = C\{b_1 \exp(-t/T_1) + b_2 \exp(-6t/T_1) + b_3 \exp(-15t/T_1)\}, \quad (1)$$

where the parameters b_i are determined by the initial conditions. The overall scaling constant C on the r.h.s. of equation (1) and the spin-lattice relaxation time T_1 are the only two fitting parameters.

The results were checked by measuring T_1 at all the other nuclear Zeeman transitions. At low temperatures, below 1 K, the quality of the fits worsenes with decreasing temperature and the functional form of the recovery of the magnetisation can be better described by a more refined analysis assuming a distribution of T_1. As this type of analysis does not change the qualitative results for $T_1^{-1}(T, H)$ we used equation (1) to analyse the recovery of the magnetisation also below 1 K.

3 Experimental results

3.1 NMR spectra of $CeAuAl_3$ in the paramagnetic phase

In Figure 2 we show three examples of ^{27}Al NMR spectra of our oriented powder of $CeAuAl_3$ (dotted lines) and the results of computer simulations (solid lines). For these

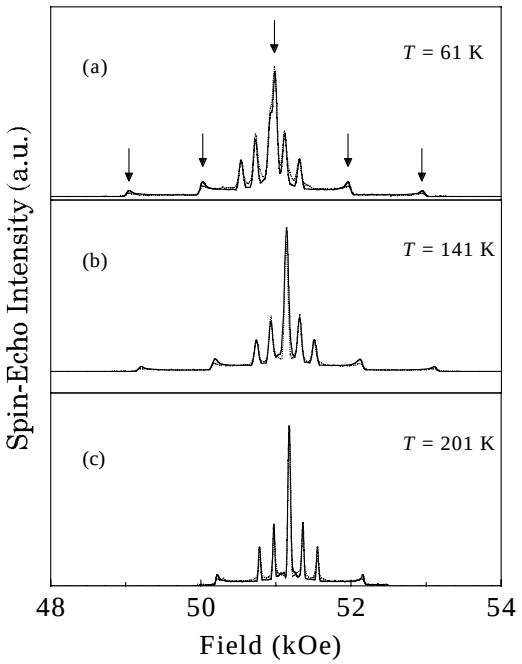

Fig. 2. The dotted curves represent the measured NMR-spectra of $CeAuAl_3$ at a frequency of 56.9 MHz for the three different temperatures 61 K, 141 K and 201 K. The solid lines represent the result of computer simulations. The arrows shown in (**a**) indicate the prominent parts of the spectrum associated with the Al_2 site, whereas the four peaks near the centre of the spectrum and the shoulder on the left side of the central line are associated with the Al_1 site.

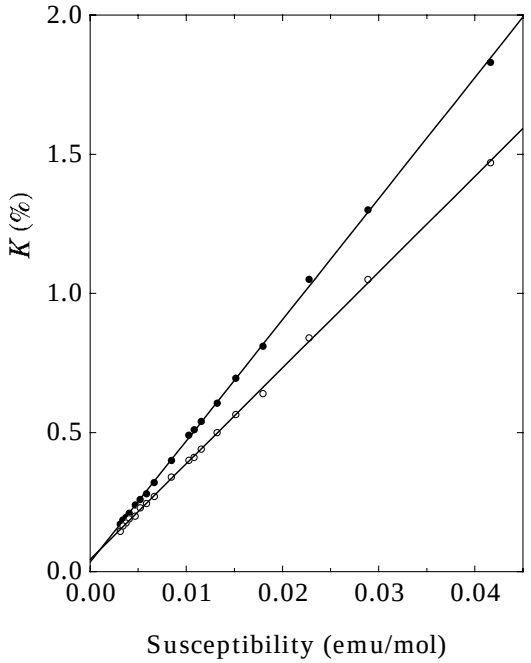

Fig. 3. The Ce $4f$-electron induced Knight shift of $CeAuAl_3$ as function of the *dc*-susceptibility, χ_f, for the Al_1 site (filled circles) and the Al_2 site (empty circles). The solid lines represent fits to the data using equation (2) (see text).

simulations the quadrupolar interaction was treated as a first- and second-order perturbation of the Zeeman term.

From the results of the simulations of our NMR-spectra we infer that more than 80% of the $CeAuAl_3$ crystallites are oriented with the *c*-axis perpendicular to the external magnetic field. This implies that the easy axis of the magnetisation is in the *ab* plane, as expected with the doublet $J_Z = \pm 1/2$ being the crystal-field ground state. For the Al_1 site we obtain the quadrupolar frequency $\nu_Q = \frac{3}{20}e^2qQ/h = 0.44 \pm 0.01$ MHz at the lowest temperatures, slightly decreasing to $\nu_Q = 0.42 \pm 0.01$ MHz at 300 K. For this site the asymmetry parameter of the electrical field gradient $\eta = \frac{V_{XX} - V_{YY}}{V_{ZZ}}$ is 0. For the Al_2 site, due to its lower symmetry (see Fig. 1), our simulations are somewhat less sensitive to the individual values of ν_Q and η. The best agreement with the experimental results is obtained for $\eta = 0.88$ and $\nu_Q = 1.17$ MHz at the lowest temperatures, slightly decreasing to $\nu_Q = 1.15$ MHz at 300 K. In this case the individual uncertainties for η and ν_Q are of the order of 20%, however, we note that from the simulations we obtain a more precise value for the product $\nu_Q(\eta + 1)$. At the lowest temperatures $\nu_Q(\eta + 1) = 2.20 \pm 0.01$ MHz.

In Figure 3 the Knight shifts K, obtained from fits to the measured NMR spectra, is plotted versus the $4f$-electron susceptibility χ_f measured on oriented $CeAuAl_3$ powder above 20 K. This plot reveals the linear relation between K and χ_f. We associate K with the transferred hyperfine coupling. Here one expects

$$K = K_0 + \frac{H_{hf}}{N_A \mu_B}\chi_f \qquad (2)$$

where H_{hf} is the transferred hyperfine coupling, *i.e.* the transferred field at the Al sites assuming $1\mu_B$ of Ce moment on each Ce site. K_0 (K_{0x}, K_{0y}, K_{0z}) is the usual Knight shift due to the Pauli paramagnetism of the conduction electrons in the absence of $4f$-electrons.

For the Al_1 site we obtain $H_{hf} = 2.40 \pm 0.01$ kOe/μ_B and $K_{0x} = K_{0y} = 360$ ppm. For the Al_2 site we obtain $H_{hf} = 1.91 \pm 0.01$ kOe/μ_B and $K_{0x} \approx K_{0y} \approx 450$ ppm. As the $CeAuAl_3$ crystallites are oriented perpendicularly to the applied magnetic field the value of K_{0z} cannot be established from our measurements. Though the measured hyperfine couplings are small compared to other similar systems, they cannot be explained by the dipolar fields of the magnetic moments of the Ce $4f$-electrons. We estimate the dipolar couplings for the Al_1 and Al_2 sites to be 0.4 kOe/μ_B and 0.3 kOe/μ_B respectively.

In Figure 4 we plot the line shift $\Delta H = H_{ref} - H_m$ of the central line ($-1/2 \leftrightarrow 1/2$) of the Al_2 site as a function of H/T in the paramagnetic regime of $CeAuAl_3$ for temperatures between 1 and 2 K. For a given frequency, H_{ref} is the resonant magnetic field for a diamagnetic reference compound and H_m is either obtained from the position of the maximum of the measured NMR spectra, or from the results of fits of the NMR spectra, of which an example is shown in the inset of Figure 4. Either procedure leads

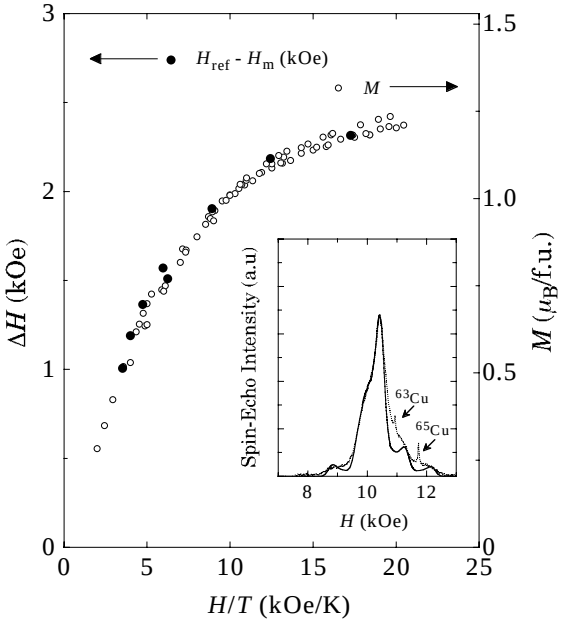

Fig. 4. NMR line shifts at the Al_2 site (filled circles) and bulk magnetisation (empty circles) for $CeAuAl_3$ powder below 2 K as a function of H/T. The resulting transfer hyperfine coupling is $H_{hf} = 1.96$ kOe/μ_B. Inset: The dotted curve represents the measured NMR spectrum of $CeAuAl_3$ at a frequency of $\nu = 13.215$ MHz and a temperature $T = 1.9$ K. From the computer simulations (solid line) we obtain the line shift at the Al_2 site that is compared with the magnetisation data.

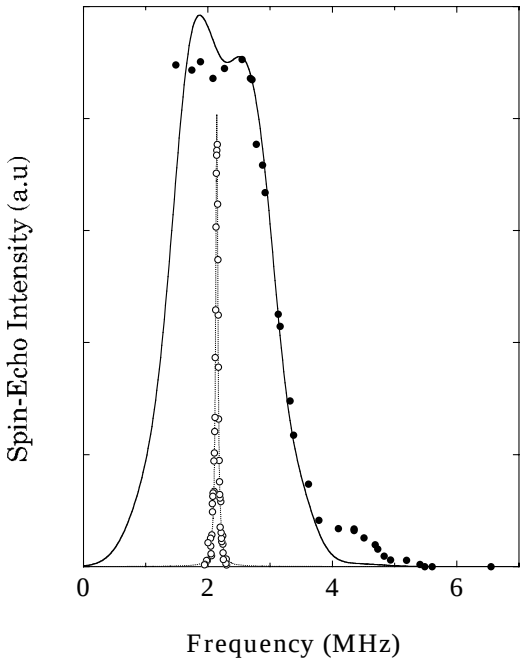

Fig. 5. Comparison of the zero field NMR spectrum of $CeAuAl_3$ (filled circles) at a temperature of 50 mK and the $LaAuAl_3$ NQR spectrum (empty circles) at a temperature of 4.2 K. The solid line represents the result of a computer simulation of the $CeAuAl_3$ data (described in the text) and the dashed line is a Lorentzian fit to the NQR spectrum of $LaAuAl_3$.

to very similar results. The ΔH values shown in Figure 4 are obtained by evaluating the maxima of the measured NMR spectra. In Figure 4 we also plot the magnetisation M (in μ_B per formula unit) data for an oriented powder [4]. It is expected that

$$\Delta H = H_{hf} M, \tag{3}$$

where H_{hf} is the transferred hyperfine coupling at the Al_2 site, and Figure 4 verifies equation (3) very nicely. We find that $H_{hf} = 1.96 \pm 0.04$ kOe/μ_B, in agreement with the result presented above, obtained by comparing the Knight shifts with the susceptibility at temperatures above 20 K. This shows that H_{hf} is temperature independent, and it also shows that our evaluation of H_{hf} is reliable.

3.2 Zero-field NMR spectrum

In Figure 5 the zero-field NMR spectrum of $CeAuAl_3$ is presented at a temperature of 50 mK, well within in the antiferromagnetically ordered state of $CeAuAl_3$. From 1.3 MHz to 2.7 MHz the NMR intensity is approximately constant, not exhibiting any distinct structures. Above 2.7 MHz the NMR intensity decreases rapidly. For comparison we have plotted the $\pm 3/2 \leftrightarrow \pm 5/2$ NQR transition at the Al_2 site of $LaAuAl_3$ where the dashed line is a Lorentzian fit function to the data with a linewidth HWHM of 22 kHz. The differences between the spectra of the Ce and the La compounds reveal the effects of the internal static fields at the Al sites present in the ordered state of $CeAuAl_3$. We have simulated the zero-field NMR spectrum of $CeAuAl_3$ by diagonalising the full Hamiltonian at the two Al sites including a quadrupole and a Zeeman term and computing the probabilities of all the transitions. In our crude model we assume a simple spiral magnetic structure where the Ce magnetic moments are aligned ferromagnetically within the ab plane and from one plane to the next along the c-axis their direction rotates by an angle δ within the ab plane. This model is based on the following: i) the easy axis of magnetisation is in the ab plane as may be concluded from the NMR signal that allows to identify the orientation of the $CeAuAl_3$ powder in an applied magnetic field, ii) compared to other Ce-compounds the hyperfine couplings are relatively small [5,6] and iii) the zero-field NMR spectrum reveals appreciable static internal magnetic fields at both Al sites. We note that a simple antiferromagnetic structure is ruled out because it would lead to well resolved lines in the zero-field NMR spectrum and this is not observed (see Fig. 5). The solid line in Figure 5 represents the result of the computer simulation.

3.3 NMR spectra of $LaAuAl_3$

In Figure 6 we show two examples of NMR spectra of $LaAuAl_3$ at a frequency of 56.9 MHz and a temperature

Table 1. NMR parameter at the Al_1 and Al_2 sites for $LaAuAl_3$ and $CeAuAl_3$. The values for the quadrupolar frequency ν_Q are given for the lowest temperatures. The values for the Knight shift of $CeAuAl_3$ K_0 are obtained by extrapolating the Knight shifts to $T = \infty$.

Site	ν_Q (MHz)	η	$\nu_Q(\eta+1)$ (MHz)	K_x (ppm)	K_y (ppm)	K_z (ppm)
$LaAuAl_3$						
Al_1	0.40 ± 0.01	0	0	600 ± 50	600 ± 50	900 ± 50
Al_2	1.11	0.58	1.76 ± 0.01	650 ± 100	650 ± 100	
$CeAuAl_3$						
Al_1	0.44 ± 0.01	0	0	360 ± 50	360 ± 50	
Al_2	1.17	0.88 (≥ 0.65)	2.20 ± 0.01	450 ± 50	450 ± 50	

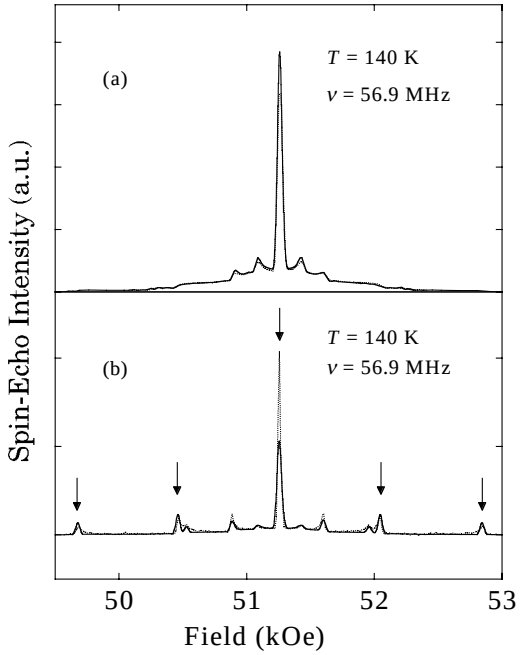

Fig. 6. The dotted curves represent the measured NMR-spectra of $LaAuAl_3$ at a temperature of 140 K and a frequency of 56.9 MHz for randomly oriented (**a**), and partially oriented powder (**b**). The solid lines represent the results of computer simulations. The arrows shown in (**b**) indicate the prominent parts of the spectrum associated with the Al_2 site, whereas the other peaks are associated with the Al_1 site.

of 140 K, for an (a) randomly and a (b) partially oriented powdered sample. The solid lines represent the simulated spectra, calculated as in the case of $CeAuAl_3$. We recall that in an external field the crystallites of $CeAuAl_3$ and $LaAuAl_3$ orient differently (Fig. 1), which results in qualitatively very different NMR spectra.

For the Al_1 site we obtain the quadrupolar frequency $\nu_Q = 0.40 \pm 0.01$ MHz at the lowest temperatures, slightly decreasing to $\nu_Q = 0.39 \pm 0.01$ MHz at 300 K. Again the asymmetry parameter η at the Al_1 site is 0, as expected from symmetry considerations. For the Al_2 site our data is consistent with $\eta = 0.57$ and $\nu_Q = 1.13$ MHz at the lowest temperatures, slightly decreasing to $\nu_Q = 1.10$ MHz at 300 K. We note that, as for $CeAuAl_3$, our result for $\nu_Q(\eta+1)$ is more precise than for ν_Q and η individually. At the lowest temperatures $\nu_Q(\eta+1) = 1.76 \pm 0.01$ MHz.

From fits to the data for the Al_1 site we obtain the isotropic Knight shift, $K_{iso} = (K_X + K_Y + K_Z)/3 = 700$ ppm $\pm$ 50 ppm, and the anisotropic Knight shift $K_1 = K_Z - K_{iso} = 200$ ppm $\pm$ 50 ppm. The Knight shift K_Z is equal to 900 ppm $\pm$ 50 ppm. All the shifts K_{iso}, K_1 and K_Z are temperature-independent.

For the Al_2 site we estimate the maximum value for the difference of K_X and K_Y to be very small. With this in mind, *i.e.*, assuming $K_X = K_Y$, we obtain for both K_X and K_Y a value of 650 ppm $\pm$ 50 ppm again not varying with temperature.

In view of a consistency check, we have also measured the NQR transitions at the Al_2 site, and found them to be at 1.48 MHz and 2.14 MHz. From these results we calculated $\nu_Q = 1.13 \pm 0.01$ MHz and an asymmetry parameter of $\eta = 0.58 \pm 0.01$, equal to the results obtained by fitting the NMR data.

We note that the electrical field gradients of $CeAuAl_3$ and $LaAuAl_3$ differ by about 10% at the Al_1 site and by about 25% at the Al_2 site. These differences are relatively large considering that both systems are expected to have similar electronic configurations except for the $4f$-electron of the Ce atom. All parameters evaluated above are summarized in Table 1.

3.4 Spin-lattice relaxation rate

In Figure 7 we present two examples of the nuclear magnetisation recovery $m(t)$ for the central transition of $CeAuAl_3$ at 56.9 MHz and 160 K, for the cases of (a) fast and (b) slow irradiation. The fits based on equation (1) for the two different irradiation conditions are of high quality and give the same value for the relaxation rate T_1^{-1}. Since we cannot resolve the contribution to the relaxation of the magnetisation for each Al site individually, our observed $T_1^{-1}(T)$ represent an average for both Al site.

In Figure 8 we present the results of the spin-lattice relaxation rate $T_1^{-1}(T, H)$ measurements as a function of T/H for $CeAuAl_3$ and $LaAuAl_3$ in the temperature range between 100 mK and 320 K.

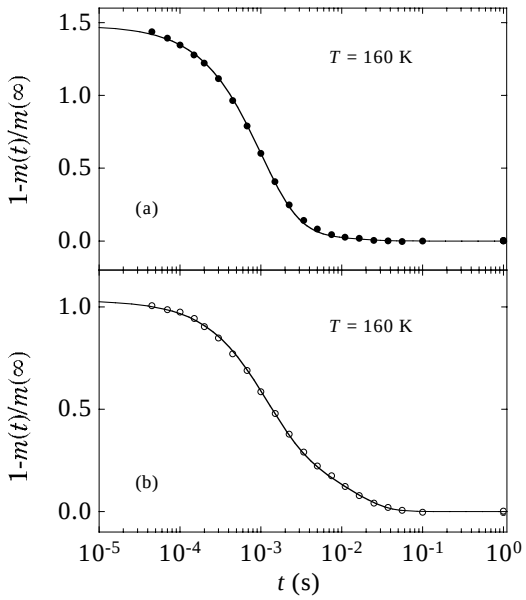

Fig. 7. Nuclear magnetisation recovery $m(t)$ for the central transition of $CeAuAl_3$ at $T = 160$ K and $\nu = 56.9$ MHz for (**a**) a fast and for (**b**) a slow irradiation. The solid lines represent fits to the data (see text). For both cases we obtain the same value of T_1^{-1}, 13.8 ± 0.1 ms^{-1}.

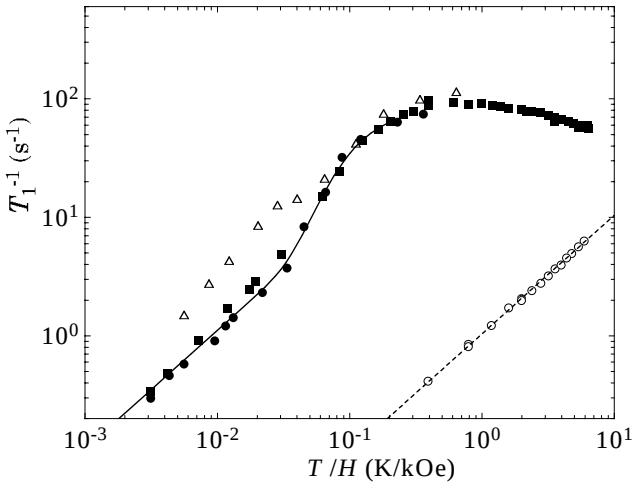

Fig. 8. $T_1^{-1}(T)$ for $CeAuAl_3$ measured at different magnetic fields ($H \approx 23$ kOe: triangles, $H \approx 47$ kOe: squares, $H \approx 67$ kOe: filled circles) and for $LaAuAl_3$ at $H = 51$ kOe (empty circles). The solid line is a guide to the eye for the high field data and the dashed line represents the linear-in-T dependence of $T_1^{-1}(T)$ for $LaAuAl_3$.

For the reference compound $LaAuAl_3$ we observe a Korringa-type linear T-dependence for the relaxation rate with $(T_1T)^{-1} = 0.02$ (sK)$^{-1}$. For $CeAuAl_3$, $T_1^{-1}(T)$ is between one and two orders of magnitude larger and less straightforward in its temperature dependence. We attribute most of the spin-lattice relaxation in $CeAuAl_3$ to be caused by Ce $4f$-moment fluctuations. In the high-temperature regime, above 20 K, $T_1^{-1}(T)$ is only weakly temperature dependent and smoothly decreases with

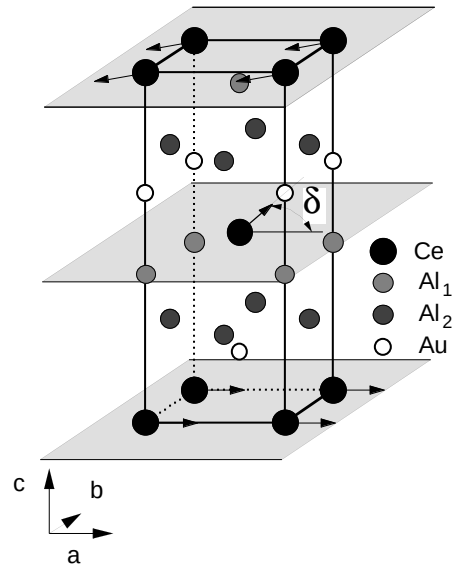

Fig. 9. Crystallographic unit cell of $CeAuAl_3$. The arrows indicate the direction of the ordered Ce moments in the antiferromagnetic state, which we propose to form a simple spiral. The moments are aligned ferromagnetically in the ab planes and from one plane to the next their direction within the basal planes is rotated by an angle $\delta = 100°$.

increasing temperatures from a value of 96 s^{-1} down to 55 s^{-1} at 320 K. Between 20 K and 1 K, the relaxation is temperature and field dependent. In particular it is inversely proportional to the applied magnetic field as may be seen in Figure 8, where the $T_1^{-1}(T)$ data for three different magnetic fields fall on a single curve when plotted as a function of T/H. In the low temperature regime below 1 K, where due to the applied magnetic field the Ce moments are ferromagnetically aligned, the temperature dependence of $T_1^{-1}(T, H)$ varies linearly with temperature, and with H^{-1} for fields above 40 kOe.

4 Discussion

4.1 NMR Spectra

As a model for the magnetic structure of $CeAuAl_3$ below 1.3 K we propose a simple spiral ordering as shown in Figure 9. In our model the Ce moments are only weakly reduced and ferromagnetically aligned within the ab planes. From one plane to the next along the c-axis the moment direction rotates by an angle δ within the ab plane. From the comparison of our measured data with the results of our simulations as discussed in Section 3.2 we infer an angle $\delta \approx 100°$ as shown in Figure 9 and a relatively small reduction of the magnetic moments of about 25%, which we associate with Kondo screening. In our simulations we considered only the nearest Ce neighbours of the Al nuclei, therefore, some discrepancies with the experimental results may be expected. More refined models which include the contribution due to interactions with the next nearest neighbours are more difficult to implement,

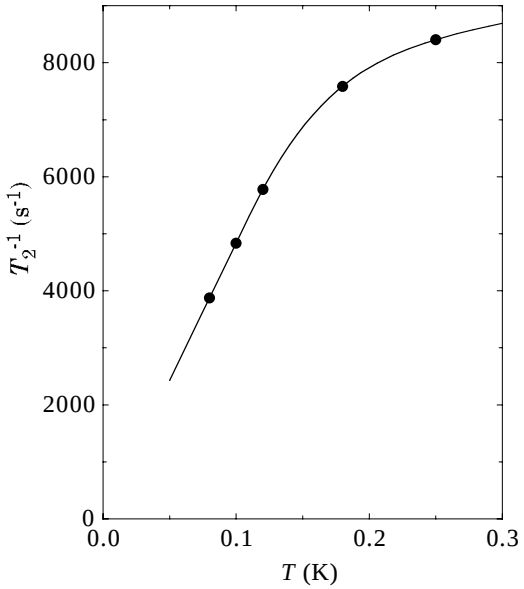

Fig. 10. Temperature dependence of T_2^{-1} measured in zero applied magnetic field at a frequency $\nu = 2.346$ MHz. The solid line is a guide to the eye.

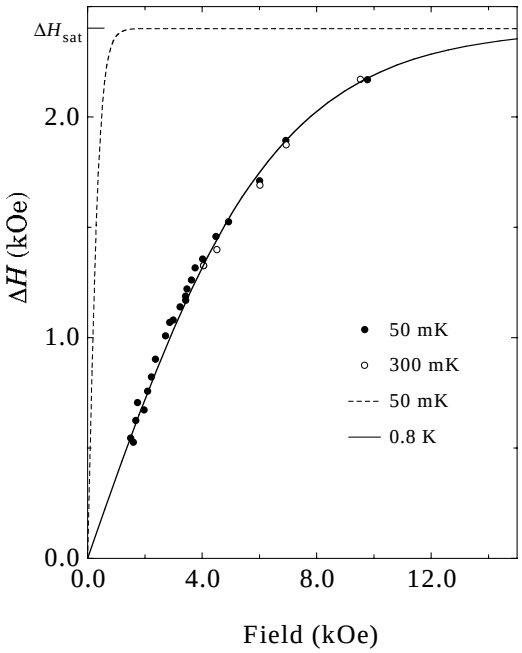

Fig. 11. Shift of the NMR line of $CeAuAl_3$ as function of the applied magnetic field for the Al_2 site at 50 mK (filled circles) and 300 mK (empty circles). The dashed and solid lines represent the expected NMR line shifts for 50 mK and 800 mK respectively, obtained using equation (3) and the measurement of the magnetisation in the paramagnetic phase (see text).

but they are not expected to yield qualitatively different results. However they might account for the small discrepancies, *e.g.*, at the highest and lowest frequencies.

Our results for the measured NMR spectra have further implications. As discussed below, the T^{-2} term in the specific heat cannot be explained by a nuclear contribution alone. From the NMR spectra of $CeAuAl_3$ we found a quadrupolar coupling constant of $e^2qQ/h = 2.9$ MHz at the Al_1 site and 7.8 MHz at the Al_2 site, corresponding to a splitting of the nuclear energy levels of $\Delta/k_B \approx 370$ μK. From the zero field NMR spectrum we estimate the internal magnetic fields at the Al sites as $H = 2.3$ and 1.2 kOe for the Al_1 and the Al_2 site, respectively. In this case, above 1 mK, C_N ought to be well described by the high temperature expansion [7]

$$C_N \approx D_2 T^{-2} \,, \tag{4}$$

where D_2 is given by

$$\frac{D_2}{R} = \frac{(2I+2)(2I+3)}{160I(2I-1)} \left(\frac{e^2qQ}{k_B}\right)^2 + \frac{(2I+2)}{6I} \left(\frac{\gamma\hbar I}{k_B}H\right)^2 , \tag{5}$$

and γ is the gyromagnetic ratio of the Al nuclei. From our NMR results we estimate D_2 to be of the order of 0.6×10^{-6} JK/mol, about two orders of magnitude smaller than the directly measured value of 41×10^{-6} JK/mol. The contribution of the Au nuclei cannot be inferred from our results, but it seems unlikely that the Au nuclei are responsible for a large contribution to the specific heat. First, the gyromagnetic ratio of Au is 15 times smaller than for Al, therefore the Zeeman contribution of the Au nuclei to C_p is expected to be much smaller than for the Al nuclei. Second, based on a simple estimate using a point charge model the Au nuclei quadrupolar contribution to C_p is also expected to be small. In principle the large excess in the observed specific heat could also be due to a precursor of yet another phase transition much below 50 mK. Further support for this conjecture may be obtained from the observed unusual strong temperature dependence of the spin-spin relaxation rate $T_2^{-1}(T)$ below 200 mK in zero applied magnetic field, as can be appreciated in Figure 10. Although we have no easy explanation for this $T_2^{-1}(T)$ behaviour, a variation of electronic interactions in the correlated system may cause the observation. We note, however, that no thermodynamic or transport property has shown any clear evidence for a second phase transition at very low temperatures down to 40 mK. Further experiments are required to clarify this issue.

In Figure 11 we present the line shift ΔH of the Al_2 site of $CeAuAl_3$ as a function of the applied magnetic field for measurements at 50 and 300 mK. The corresponding Larmor frequencies of the low-field measurements are very small and, combined with the small T_2, results in very poor signal-to-noise ratios. For this reason low-field measurements above 0.3 K were not practical. The curves in Figure 11 are the expected NMR line shifts at 50 mK (dashed line) and 800 mK (solid line) using equation (3) and scaling the $M(H)$ data from the measurement of the bulk magnetisation in the paramagnetic phase [4]. It may be seen that the calculated curve for $T = 800$ mK fits very well the data for $T = 300$ and 50 mK, respectively. Thus, below 300 mK the line shift displays no noticeable temperature dependence, but it varies strongly with the ap-

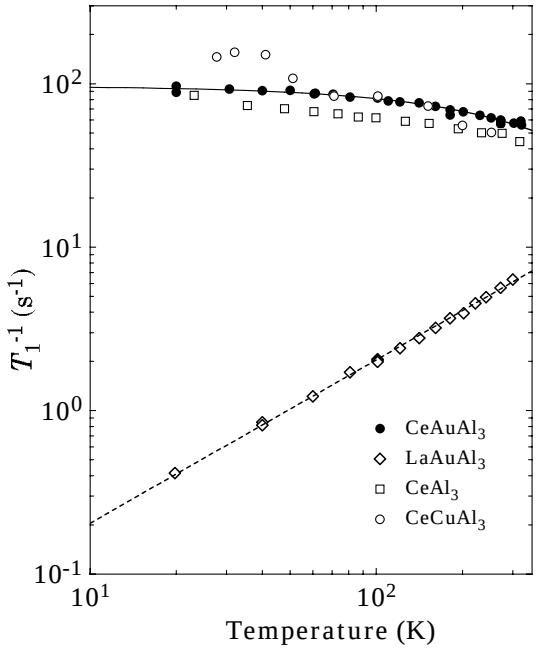

Fig. 12. Temperature dependence of $T_1^{-1}(T)$ for $CeAuAl_3$ (filled circles), $LaAuAl_3$ (empty diamonds), $CeCuAl_3$ (empty circles) [12] and $CeAl_3$ (empty squares) [11]. The solid line is a guide to the eye for the $CeAuAl_3$ data and the dashed line shows the Korringa behaviour of the $LaAuAl_3$ data.

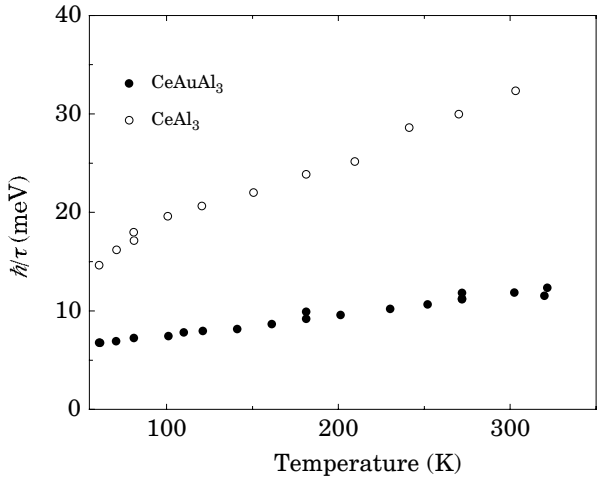

Fig. 13. Temperature dependence of the Ce-spin fluctuation rate for $CeAuAl_3$ (filled circles) and $CeAl_3$ (empty circles) [11].

plied magnetic field. The curves shown in Figure 11 imply that no T-dependence of ΔH occurs below 800 mK. Our results are consistent with the expectations for antiferromagnets in magnetic fields, where the transverse magnetic susceptibility is temperature independent at low temperatures. This is especially the case for spiral magnetic structures [8,9].

4.2 Spin-lattice relaxation rate

Above 20 K the temperature dependence of the relaxation rate $T_1^{-1}(T)$ of $CeAuAl_3$ is very similar to that of other Ce intermetallic compounds, such as $CeAl_2$ [10], $CeAl_3$ [11] and $CeCuAl_3$ [12], as is demonstrated in Figure 12. The crystal-field effects, due to excited doublets at 58 K and 265 K for the case of $CeAuAl_3$ [2], are not evident in the relaxation rate in an unambiguous way. In the high temperature regime the relaxation rate is dominated by the weakly interacting Ce moments. We note that for a T-independent transferred hyperfine coupling, consistent with the results of our measurements, and assuming in addition that the Ce-spin fluctuation rate $1/\tau$ is temperature independent, the relaxation rate is expected to be T-independent. As shown in Figure 12 this is not really the case for $CeAuAl_3$. In fact the temperature dependence for $1/\tau$ may be obtained from [10]

$$1/\tau = 2N_{\rm A}\gamma_n^2 k_B K^2 T_1 T/\chi. \qquad (6)$$

The results for $1/\tau$ are displayed in Figure 13 where, as a reference, we have also plotted $1/\tau$ for $CeAl_3$ [11]. We observe that the Ce-spin fluctuation rate for $CeAuAl_3$ is smaller than for the heavy-electron compound $CeAl_3$. Therefore one might expect a relatively smaller hybridization of the f-electrons with the conduction electrons at low temperatures for $CeAuAl_3$ than for $CeAl_3$. In fact this is consistent with an incomplete Kondo screening of the order of only about 25% estimated for $CeAuAl_3$.

A way for estimating the enhancement of the relaxation rate T_1^{-1} due to the presence of the $4f$-electrons in the high-T regime of a Kondo system was suggested by Fradin [13] and later generalized by Crisan [14]. This model calculation yields $T_1^{-1} \approx 1.6$ s^{-1} which is about 50 times smaller than the measured relaxation rate, underlining the difficulties associated with estimates of the spin-lattice relaxation rate in metallic systems.

In the low temperature regime, below 1 K, applied external magnetic fields H exceeding 23 kOe change the antiferromagnetic phase into a paramagnetic phase, *i.e.*, an induced ferromagnetic phase. This may be appreciated in Figure 11 where the saturation level ΔH_{sat} is practically achieved at 800 mK for fields above 15 kOe. It is interesting to see (Fig. 8) that in these temperature and field ranges the linear-in-T term of $T_1^{-1}(T)$, for fields of a few tens of kOe, is still two orders of magnitude larger than for the reference compound $LaAuAl_3$ and T_1^{-1} scales with T/H. However for lower fields ($H < 30$ kOe) an extra enhancement in the relaxation rate is observed.

The spin-lattice relaxation rate $T_1^{-1}(T)$ of $LaAuAl_3$ follows a linear-in-T dependence. The value of $(T_1T)^{-1}$ is 0.02 (sK^{-1}), about 30 times smaller than for Aluminum metal, even though both materials have similar linear-in-T contributions, γ, to the specific heat. The low value of $(T_1T)^{-1}$ for $LaAuAl_3$ must therefore be attributed to an extremely small hyperfine coupling.

5 Summary

For the magnetically ordered state of the new heavy-electron antiferromagnet $CeAuAl_3$ we propose a model for the magnetic structure, where the magnetic moments are only weakly reduced by Kondo screening. This magnetic structure is a simple spiral where the Ce ordered moments are aligned ferromagnetically in the ab planes and from one plane to the next along the c-axis their direction rotates within the ab planes. In the high temperature regime the temperature dependence of the relaxation rate $T_1^{-1}(T)$ is shown to be similar to other heavy-electron Ce compounds and at low temperatures $T_1^{-1}(T,H)$ is found to be field dependent and strongly enhanced compared to the reference compound $LaAuAl_3$. Our results are consistent with a $4f$-moment reduction of the order of 25%, which we associate with an incomplete Kondo screening. The results for $T_1^{-1}(T)$ suggest the presence of low energy excitations in the f-electron system at low temperatures, especially for low magnetic fields. The observed $a_N T^{-2}$ term in $C_p(T)$ at very low temperatures cannot be accounted for by a nuclear contribution, considering our results for the quadrupolar coupling constants and the estimated static internal fields at the Al sites of $CeAuAl_3$. This may be a hint for a phase transition of unknown nature at very low temperatures, not indicated by any of the thermal and transport properties [2]. Further support for this conjecture is obtained from our results for $T_2^{-1}(T)$.

We thank S. Sigrist for the sample synthesis and D. Rau for his help in some parts of the project. This work was in part financially supported by the Schweizerische Nationalfonds zur Förderung der Wissenschaftlichen Forschung.

References

1. F. Hulliger, J. Alloys & Compounds **218**, 255 (1995).
2. S. Paschen, E. Felder, H.R. Ott, Eur. Phys. J. B **2**, 169 (1998).
3. A. Narath, Phys. Rev. **162**, 320 (1967).
4. S. Paschen, private communication.
5. J.L. Gavilano, P. Vonlanthen, B. Ambrosini, J. Hunziker, F. Hulliger, H.R. Ott, Europhys. Lett. **32**, 361 (1995).
6. P. Vonlanthen, J.L. Gavilano, B. Ambrosini, D. Heisenberg, F. Hulliger, H.R. Ott, Z. Phys. B **102**, 347 (1997).
7. N.E. Phillips, CRC Critical Reviews in Solid State Sciences 467 (1971).
8. T. Nagamiya, K. Nagata, Y. Kitano, Prog. Theor. Phys. **27**, 1253 (1962).
9. Y. Kitano, T. Nagamiya, Prog. Theor. Phys. **31**, 1 (1964).
10. D.E. MacLaughlin, O. Pea, M. Lysak, Phys. Rev. B **23**, 1039 (1981).
11. M.J. Lysak, D.E. MacLaughlin, Phys. Rev. B **31**, 6963 (1985).
12. S. Aoyama, H. Ido, T. Nishioka, M. Kontani, Czech. J. Phys. **46-S4**, 2069 (1996).
13. F.Y. Fradin, J. Phys. Chem. Solids **31**, 2715 (1970).
14. M. Crisan, Phys. Lett. A **115**, 69 (1986).